Estimating Noise Levels of Remotely Sensed Measurements from Satellites Using Spatial Structure Analysis

DONALD W. HILLGER AND THOMAS H. VONDER HAAR

Cooperative Institute for Research in the Atmosphere (CIRA), Colorado State University, Fort Collins, Colorado

(Manuscript received 29 January 1987, in final form 24 August 1987)

ABSTRACT

A technique is presented whereby the noise level of satellite measurements of the atmosphere and earth can be estimated. The technique analyzes a spatial array of data measured by a satellite instrument. A minimum of about 200 satellite measurements is required, preferably in a regular pattern. Statistical structure analysis is used to describe a combination of the mean gradient and noise in the data. The noise level is then estimated by separating out the gradient information and leaving only the noise. Results are presented for four satellite sounding instruments, and effective blackbody or brightness temperature noise levels were compared to prelaunch specifications or inflight calibrations for each instrument. Comparisons showed that in the absence of cloud-contaminated measurements (in the case of infrared data) and away from the highly variable ground surface, the noise level of various satellite instruments can be obtained without the need for calibration data. The noise levels imply how much spatial averaging is *possible*, without smearing the detected geophysical gradient, and how much is *necessary*, to meet the absolute signal accuracy requirements for the intended use of the satellite measurements.

1. Introduction

For many purposes it is desirable to know the noise level of remotely sensed measurements of the atmosphere and earth as obtained from satellite-borne instruments. This type of information is usually available from pre-launch testing or inflight calibration sequences. However, instrument noise levels may change with time and calibration data are sometimes not available to the user. There is an alternative, statistical method of obtaining the effective instrument noise level of satellite measurements. That method is to employ structure analysis of spatial arrays of operational satellite measurements. By using structure analysis on these measurements a statistical combination of the mean gradient plus noise is estimated. The gradient in most cases can be separated from the noise component of the structure function. Hillger and Vonder Haar (1979) applied these analysis techniques to data from the Vertical Temperature Profile Radiometer (VTPR). Results of the same method, except with emphasis on noise level estimation, are computed for current satellite instruments and are compared to noise levels obtained by more conventional means.

2. Spatial structure analysis

The spatial structure is the mean-squared difference between paired measurements as a function of their separation distance. The structure is computed from all possible combinations of paired measurements. Discrete structure values are obtained by grouping the paired measurements according to their separation distance. The resultant structure function generally increases with distance (on scales small relative to the observed phenomena) since each computed structure value contains geophysical gradient information as well as noise. Removal of the gradient component of the statistic is possible by extrapolating the structure to zero separation distance. Since there is no gradient at zero distance, only the noise remains. The extrapolation compensates for the fact that spatially coincident measurements are generally not available and results in an indirect way of determining the noise level in satellite measurements. Details of the computation of the structure function for satellite data are explained by Hillger and Vonder Haar (1979). Fuelberg and Meyer (1986) used the same technique to determine the noise levels of meteorological parameters retrieved from atmospheric sounding measurements.

The spatial structure can be computed either one- or two-dimensionally. The one-dimensional structure can be computed assuming isotropy (independence with respect to directional orientation) or can be computed in a specified orientation. In the case of satellite data the orientation is a fundamental consideration. Most satellite measurements are gathered in scan lines composed of individual elements. The spacing of the measurements between lines can differ from the spacing between elements. Also, there is a limb effect for mea-

Corresponding author address: Dr. Don Hillger, NOAA/NESDIS/RAMM Branch, CIRA/Colorado State University, Foothills Campus, Fort Collins, CO 80523-0033.

surements taken at varying zenith angles with respect to the earth.

One way to avoid the limb (darkening or brightening) effect is to compute the structure using measurements at constant zenith angles. For low-earth-orbit (polar-orbiting) satellites, that is possible by pairing measurements from one scan line to the next, at equal element positions on the scan line. Figure 1 shows an example of polar-orbiting satellite measurement locations on the earth. A preferred orientation, therefore, is to compute the structure along the elements. The horizontal spacing of the measurements in the element orientation is fairly constant.

a. Structure formulation

The structure function as defined by Gandin (1963) can be applied directly to pairs of measurements at fixed locations. However, in the case of satellite data, there are no fixed locations at which measurements are obtained. Therefore, the definition of the structure function was modified for this type of data (Hillger and Vonder Haar, 1979). Instead of computing the structure between a unique pair of locations, discrete structure values are calculated for all possible pairs of measurements with separation distances between assigned limits. Summations are made for all pairs of measurements with similar separation distances, and discrete structure values are computed at all separation distances appropriate to the spacing and coverage of the satellite measurements.

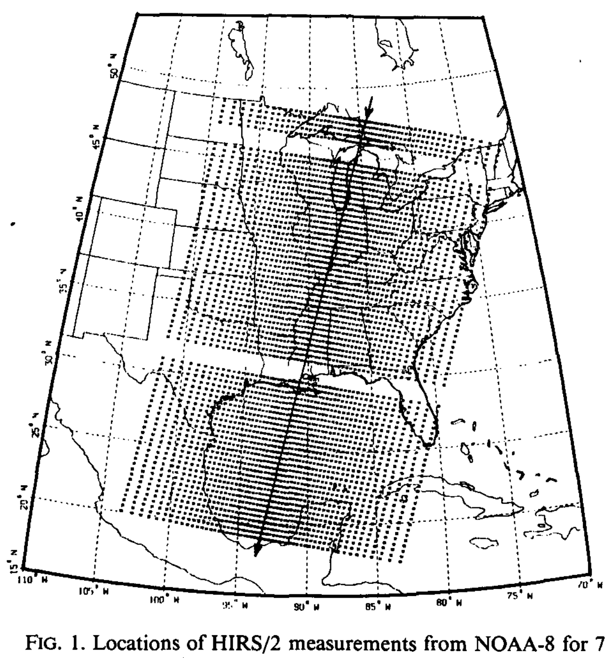

FIG. 1. Locations of HIRS/2 measurements from NOAA-8 for 7 June 1984 at approximately 1400 UTC. Scan lines are approximately perpendicular to the subsatellite track (given by the arrows). Note the nearly constant spacing in the element orientation, but not along the scan lines.

One assumption is necessary to apply the structure function to a horizontal field of satellite measurements. That assumption is that the field is homogeneous with respect to the structure function. In other words, the statistical relationship between paired measurements should be independent of translation of the measurement locations. This assumption allows a large statistical base to be accumulated from a relatively small number of measurements. A minimum of about 200 measurements is recommended, resulting in about 20 000 combinations, or pairs, of measurements.

To illustrate for a spatial array of data, if each satellite measurement T (e.g., temperature) can be identified by a given line i and element j, then the structure can be computed in the element orientation such that

$$STR(k) = \sum_{i,j} [T(i,j) - T(i+k,j)]^2/N(k), \quad (1)$$

where k is the line increment and $N(k)$ is the number of pairs for a given k. A discrete structure value is computed for each line increment k from 1 to one less than the maximum number of lines. However, the determination of the structure values is based on separation distances and not solely on line increments. The actual formulation is slightly complicated by the fact that the satellite measurement locations on the earth are not exactly an equally spaced grid. The satellite measurement positions, however, are regular enough to allow the above formulation if the distances at which the structure is computed are equal to the average spacing of the satellite measurements. Figure 2 shows an example of a structure function (discrete structure values) computed for satellite measurements in the element orientation.

b. Estimating noise using structure analysis

Each measurement from the satellite contains a noise component (error) such that

$$T(i,j) = T^*(i,j) + e(i,j), \quad (2)$$

where e is the error in T and T^* is the noiseless measurement. Gandin (1963) showed that the structure function at all distances is thus exaggerated by twice the mean-squared error,

$$STR(d) = STR^*(d) + 2\sigma^2, \quad (3)$$

where

$$\sigma^2 = \overline{e^2}.$$

In this case the structure function is given in terms of separation distance d instead of line increment k.

The discrete structure values computed at each distance or line increment ($k = 1, 2, 3, \cdots$) have both a mean-squared difference (gradient) and an error component. However, at zero separation distance ($k = 0$) there is no gradient, so only the noise remains. At $d = 0$, $STR^*(d = 0) = 0$ and $STR(d = 0) = 2\sigma^2$. Therefore, the root mean square error can be estimated

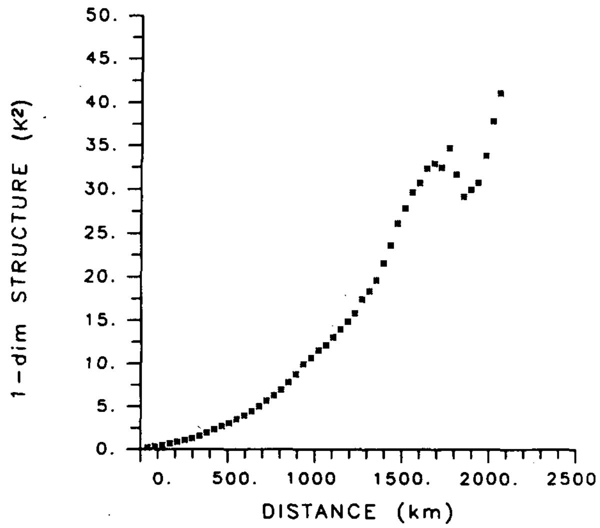

FIG. 2. Structure function (discrete structure values) for HIRS/2 channel 15 (4.46 μm) as computed in the element orientation. Data were from NOAA-7 on 28 March 1984 at approximately 2100 UTC. The line spacing is about 42 km.

by extrapolating the structure function to zero distance. The extrapolation process, however, may yield different estimated noise levels depending on the functional form used in the extrapolation.

c. Extrapolating the structure function

Various functions can be easily fitted to the discrete structure values. Polynomials up to the fourth order were used in the present study, with each polynomial fitted to the structure values using least-squares techniques. The polynomial forms selected for use are given in Table 1. Instead of total freedom in selecting the coefficients (A through E), certain restrictions were imposed. The primary restriction was that the second polynomial coefficient must be zero ($B = 0$), which means that the gradient (slope or first derivative) is zero at zero distance. By definition the derivative of the structure function is zero at zero distance. A second restriction was that the first nonzero coefficient must be positive ($C > 0$). This assures that the fitted polynomial is an increasing function (positive second derivative) at small distances. The minimum in the fitted polynomial should occur at the extrapolated intercept and not between the extrapolated intercept and the structure value at the minimum distance between satellite measurements. A third restriction was that the intercept be greater than zero ($A > 0$). This assures that the noise level is not imaginary, since it is proportional to the square root of the intercept.

TABLE 1. Fitted polynomials with zero slope at $d = 0$ for $STR(d) = A + Bd + Cd^2 + Dd^3 + Ed^4$.

	Coefficient					Number
Name	A	B	C	D	E	of nonzero coefficients
Second-order	$A > 0$	$B = 0$	$C > 0$	—	—	2
Third-order	$A > 0$	$B = 0$	$C > 0$	D	—	3
Fourth-order	$A > 0$	$B = 0$	$C > 0$	D	E	4

Fitted polynomials were weighted by the number of pairs contributing to each structure value and inversely by the mean separation distance. These weights caused the polynomials to be fitted more closely to the structure values nearest to zero separation distance. For each set of structure values, polynomials were fit to a varying number of values, with a preference for fits to large numbers of values. Figure 3 shows an example of polynomials fitted to discrete structure values for a different satellite channel than in Fig. 2. The polynomials are zero-slope second-, third-, and fourth-order. All three extrapolations in this case gave similar intercepts, as was true in many situations. The intercept from the polynomial with the highest coefficient of determination (or highest explained variance) and meeting the above restrictions was chosen as the estimated noise. This value is used in all the following results.

3. Satellite instruments analyzed

Data from four satellite sounding instruments were analyzed. Table 2 gives pertinent information on all the measurements and limited details on the analysis procedure for each. Two of the instruments measure in the infrared: the High-resolution Infrared Radiation Sounder (HIRS/2) on NOAA satellites and the VISSR Atmospheric Sounder (VAS) on GOES. The other two

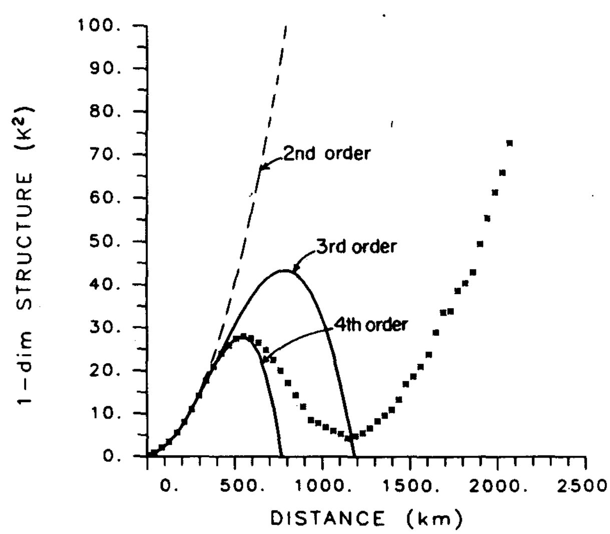

FIG. 3. As in Fig. 2 except for HIRS/2 channel 11 (7.3 μm). Three polynomials were fitted to the structure values to determine the structure at zero distance. Weighting was used to force the polynomials to be fitted more closely to the structure values nearest to zero separation distance.

TABLE 2. Satellite instruments.

Satellite	Orbit	Instrument	Spectral band	Structure orientation	Spatial resolution (km)	Date(s)	Number of measurements
NOAA-7	polar	HIRS/2	infrared	element	42.6	28 Mar 1984	1635
NOAA-8	polar	HIRS/2	infrared	element	42.7	7 Jun 1984	2066
NOAA-7	polar	MSU	microwave	element	169.6	28 Mar 1984	231
NOAA-8	polar	MSU	microwave	element	170.5	7 Jun 1984	209
DMSP	polar	SSM/T	microwave	element	213.3	26 Oct 1985–21 Dec 1985	8971
GOES-5	geosynchronous	VAS	infrared	line	13.5	7 Sep 1985	1132
GOES-5	geosynchronous	VAS	infrared	element	23.3	7 Sep 1985	1132

instruments measure in the microwave: the Microwave Sounding Unit (MSU) on NOAA and the Special Sensor for Microwave Temperature (SSM/T) on Defense Meteorological Satellite Program (DMSP) satellites. For HIRS/2 and MSU, data from two satellites were analyzed. All of the polar-orbiting satellite data were analyzed in the element orientation to avoid problems with variations in scan angle (limb effects). However, the geosynchronous VAS data were analyzed independently in both the line and element orientations, since the scan angle variations were small.

All datasets consisted of measurements primarily over the continental United States. In the case of measurements from polar orbit, the area of consideration was quite large (see Fig. 1). For higher resolution measurements from geosynchronous orbit, the analysis region was much smaller (see Fig. 4). The resolution of the structure analysis as given in Table 2 is the average separation distance between measurements in the given orientation. All measurements were available as either effective blackbody temperatures (infrared) or brightness temperatures (microwave).

4. Estimated noise results

a. High-resolution Infrared Radiation Sounder (HIRS/2)

The noise results estimated from structure analysis of HIRS/2 are given in Table 3. The equation $\sigma = [STR(d)/2]^{1/2}$ was solved at two points along each structure curve: at the minimum measurement separation distance (d = minimum) and at zero distance ($d = 0$) using extrapolated values of structure. The first solution assumes that the structure function is at its minimum at d = minimum, which generally is not true since a gradient exists between measurements at finite separation distance. The second (extrapolated) solution will be less than the first solution (in all but no-gradient situations) and should have most of the gradient removed (except in the cases of strong cloud or surface contribution).

The structure-estimated noise levels are compared to prelaunch specifications (Schwalb, 1978). The prelaunch specifications were originally given in terms of noise equivalent radiance differences but were converted into noise equivalent temperature differences (NEΔTs) by using the Planck function and the mean temperature observed in each channel. Werbowetzki (1981) also lists NEΔTs which differ slightly from those in Table 3.

The last two columns in Table 3 give the ratios of noise levels (extrapolated vs NEΔT). The noise levels compare favorably for HIRS/2 channels 1–4, 11, 12, 16, and 17. Ratios between the estimated and NEΔT noise levels for these channels are within the range 0.4 to 1.4 (about a factor of 2). For most of the other HIRS/2 channels, however, the ratios are much greater than 2.0. This is most likely caused by cloud and ground surface effects on the measurements that were used. Clouds and surface variations occur on spatial scales much smaller than the satellite resolution, so extrapolation cannot possibly eliminate all the gradient contribution. An attempt was made to eliminate cloud-contaminated HIRS/2 measurements by using a maximum threshold value for the 11-μm window (channel 8) and a minimum threshold value for 0.7-μm reflected visible radiation (channel 20). This cloud-elimination method, however, was not effective, which presents a problem for structure analysis. The structure-estimated

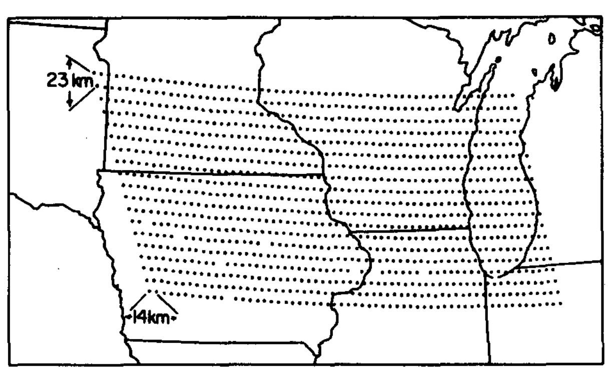

FIG. 4. Locations of VAS measurements from GOES-5 for 7 Sept 1983 at approximately 1400 UTC. Portions of 19 scan lines with up to 60 elements in each are shown.

TABLE 3. Noise levels from structure analysis of HIRS/2 effective blackbody temperatures from NOAA-7 (1635 FOVs) and NOAA-8 (2066 FOVs).

		Estimated noise						
		Minimum distance (d = 43 km)		Extrapolated (d = 0 km)			Noise ratio (Extrapolated vs NEΔT)	
HIRS/2 channel	Wavelength (μm)	NOAA-7 (K)	NOAA-8 (K)	NOAA-7 (K)	NOAA-8 (K)	NEΔT* (K)	NOAA-7	NOAA-8
1	15.0	0.70	0.78	0.70	0.70	0.75	0.9	0.9
2	14.7	0.19	0.20	0.15	0.19	0.30	0.5	0.6
3	14.5	0.18	0.21	0.14	0.20	0.30	0.5	0.7
4	14.2	0.20	0.38	0.17	0.31	0.22	0.8	1.4
5	14.0	0.38	0.79	0.30	0.67	0.19	1.6	3.5
6	13.7	0.53	1.08	0.41	0.92	0.17	2.4	5.4
7	13.4	0.75	1.45	0.55	1.29	0.15	3.7	8.6
8	11.1	1.10	1.99	0.75	1.77	0.07	10.7	25.3
9	9.7	0.76	1.14	0.49	1.02	0.14	3.5	7.3
10	8.3	0.80	1.38	0.54	1.22	0.16	3.4	7.6
11	7.3	0.67	0.84	0.37	0.49	0.47	0.8	1.0
12	6.7	0.63	0.80	0.48	0.36	0.49	1.0	0.7
13	4.57	0.68	1.09	0.46	0.96	0.03	15.3	32.0
14	4.52	0.47	0.84	0.32	0.77	0.06	5.3	12.8
15	4.46	0.26	0.54	0.19	0.48	0.11	1.7	4.4
16	4.40	0.14	0.18	0.12	0.17	0.34	0.4	0.5
17	4.24	0.10	0.11	0.08	0.09	0.19	0.4	0.5
18	4.0	1.11	1.02	0.71	0.73	0.05	14.2	14.6
19	3.7	1.36	1.23	0.98	1.06	0.04	24.5	26.5

* NEΔT = noise equivalent temperature difference (Schwalb, 1978).

noise levels for channels with peak contribution from the lower troposphere (HIRS/2 channels 5–10, 13–15, 18 and 19) are much greater than the NEΔTs for those channels. All other noncloud contaminated channels seem to be performing near or below NEΔT requirements.

b. Microwave Sounding Unit (MSU)

In order to test the method in the absence of clouds, microwave measurements are the answer. For microwave measurements the only cloud influence should be from large cloud droplets or rain. These measurements therefore avoid many of the problems encountered by cloud-contaminated infrared measurements.

Results for MSU are given in Table 4. In this case the extrapolated noise levels for data from the two satellites are compared to the specified maximum NEΔTs for the MSU (Schwalb, 1978). Again, the last two columns in Table 4 give the ratios of the extrapolated noise levels to the maximum NEΔTs. Ratios are 1.0 or less, with the structure-estimated noise less than the maximum NEΔTs for MSU channels 2, 3, and 4. Another set of noise levels for a particular instrument (Swanson et al., 1980) is given under the NEΔT column. These NEΔTs compare especially well with the extrapolated noise levels for NOAA-7 MSU channels 2, 3, and 4. In contrast, MSU channel 1 has a large surface emittance contribution, which causes effects similar to high-resolution cloud variations. Therefore,

TABLE 4. Noise levels from structure analysis of MSU brightness temperatures from NOAA-7 (231 FOVs) and NOAA-8 (209 FOVs).

		Estimated noise							
		Minimum distance (d = 170 km)		Extrapolated (d = 0 km)		NEΔT*		Noise ratio (extrapolated vs max NEΔT)	
MSU channel	Frequency (GHz)	NOAA-7 (K)	NOAA-8 (K)	NOAA-7 (K)	NOAA-8 (K)	Max (K)	Unit-4 (K)	NOAA-7	NOAA-8
1	50.3	6.79	7.38	3.59	4.97	0.3	0.21	12.0	16.6
2	53.7	0.71	0.37	0.24	0.30	0.3	0.22	0.8	1.0
3	55.0	0.41	0.26	0.19	0.19	0.3	0.18	0.6	0.6
4	57.1	0.59	0.42	0.22	0.13	0.3	0.21	0.7	0.4

* NEΔT = noise equivalent temperature difference [Maximum (Schwalb, 1978), MSU unit-4 (Swanson, et al., 1980)].

the structure function for MSU channel 1 cannot be extrapolated to give a noise estimate which compares favorably to the specified NEΔT for that channel.

c. Special Sensor for Microwave Temperature (SSM/T)

The results for DMSP SSM/T microwave sounding measurements were expected to be similar to those for the MSU. Table 5 gives a comparison of the extrapolated noise vs specified maximum NEΔTs (Aerojet, 1977; Grody et al., 1985). Noise ratios in the last column are within the range 0.5 to 1.0 for SSM/T channels 2 through 7, with the structure-estimated results less than the specified NEΔTs. Like MSU, these higher-numbered channels have their peak contribution above the surface. The SSM/T channel 1 is a microwave window channel which is affected by high-resolution surface emittance and temperature variations, and like MSU, the extrapolated noise level is much larger than the specified NEΔT.

d. VISSR Atmospheric Sounder (VAS)

The VAS measurements, like HIRS/2, were from the infrared spectrum and are susceptible to cloud contamination. However, the VAS spatial resolution (~14 km) is higher than that of HIRS/2 (~43 km). The visible channel on GOES was used to aid in the cloud detection. Data were selected from a region which was judged to be cloud free by inspection of 1-km visible imagery.

Table 6 gives the estimated noise levels from a structure analysis computed independently in both the line and element orientations. Both orientations may be used because of small variations in scan angle (and, therefore, small variations in limb effects) among the VAS measurements for the relatively small area considered. One difference between the two structure orientations is the spacing of the VAS measurements, as can be seen in Fig. 4, and the resultant spacing of the discrete structure values. The average data spacing in the element measurement is larger (~23 km) than in the line orientation (~14 km). This results in the noise estimates at minimum distance being greater in the element orientation than in the line orientation since more gradient information remains at larger distances. The extrapolated noise levels also were greater in the element orientation, although the extrapolation process ideally should have eliminated all of the gradient in the structure function and would have resulted in identical noise levels.

The most likely explanation for the differences in noise levels between the two orientations is the sampling order of the measurements. Since the measurements are successively sampled along scan lines there is a correlation between closely spaced measurements due to slow electronic sampling or memory. This causes along-line measurements to be more correlated than along-element measurements, resulting in lower estimated noise levels for along-line analysis than for along-element analysis. Differences between extrapolated noise levels for the two orientations give an indication of the stability of the results. Some discrepancy is reasonable since the noise levels are estimates based on limited data.

Extrapolated noise results are compared to inflight single-sample noise (SSN) estimates for GOES-5 (Menzel et al., 1983). Chesters and Robinson (1983) and Smith (1983) also list inflight SSN levels which differ slightly from those in Table 6. Noise ratios (extrapolated vs SSN) are within the range 0.8 to 1.8 (a factor of 2) for all but VAS channel 8, which is a window channel. (No data were available from VAS channel 11.) Even for many lower-tropospheric channels the structure-estimated noise levels are not greatly exaggerated (note especially VAS channels 5, 7 and 12). The good agreements with inflight SSN values show that the structure-estimated noise can be quite reliable when cloud-contaminated measurements are eliminated from infrared data. [For channels with very little surface contribution (VAS 2–4, 9, 10) the agreement is excellent.] Only for the window channels (VAS channel 8 and possibly channel 12) are the structure-estimated noise levels much greater than the single-sample noise values.

TABLE 5. Noise levels from structure analysis of DMSP SSM/T brightness temperatures for 26 Oct–21 Dec 1985 (26 days, 8791 FOVs).

		Estimated noise			
SSM/T channel	Frequency (GHz)	Minimum distance (d = 213 km) (K)	Extrapolated (d = 0 km) (K)	Maximum NEΔT* (K)	Noise ratio (extrapolated vs NEΔT)
1	50.5	5.77	2.10	0.6	3.5
2	53.2	1.25	0.38	0.4	1.0
3	54.4	0.60	0.27	0.4	0.7
4	54.9	0.32	0.20	0.4	0.5
5	58.4	0.92	0.31	0.5	0.6
6	58.8	0.58	0.31	0.4	0.8
7	59.4	0.57	0.32	0.4	0.8

* NEΔT = noise equivalent temperature difference (Aerojet, 1977; Grody et al., 1985).

TABLE 6. Noise levels from structure analysis of GOES-5 VAS effective blackbody temperatures for 7 Sep 1983 (1132 FOVs).

		Estimated noise							
		Minimum distance		Extrapolated				Noise ratio (extrapolated vs SSN)	
		(*d* = 14 km)	(*d* = 23 km)	(*d* = 0 km)					
VAS channel	Wavelength (μm)	line (K)	element (K)	line (K)	element (K)	Spin budget	Inflight SSN* (K)	line	element
1	14.7	2.79	3.05	2.78	3.05	1	2.28	1.2	1.3
2	14.5	0.82	0.94	0.81	0.93	3	0.93	0.9	1.0
3	14.3	0.55	0.61	0.53	0.60	4	0.64	0.8	0.9
4	14.0	0.53	0.60	0.51	0.58	3	0.52	1.0	1.1
5	13.3	0.49	0.56	0.43	0.50	2	0.40	1.1	1.3
6	4.5	0.34	0.42	0.30	0.35	6	0.22	1.4	1.6
7	12.7	0.46	0.53	0.33	0.38	2	0.28	1.2	1.4
8	11.2	0.41	0.47	0.16	0.27	1	0.06	2.7	4.5
9	7.3	0.82	0.91	0.77	0.88	3	0.83	0.9	1.1
10	6.8	0.67	0.79	0.61	0.76	1	0.72	0.8	1.1
11	4.4	na†	na	na	na	0	1.95	na	na
12	3.9	0.45	0.53	0.32	0.35	1	0.19	1.7	1.8

* SSN: single sample noise (Menzel et al., 1983) adjusted for spin budget and converted from radiance to temperature units.
† na data not available.

5. Requirements for spatial averaging of VAS measurements

a. Possible averaging

There are two ways to look at noise levels in terms of what they imply about spatial averaging of VAS data. One way is to look at the averaging that may be *possible* without smearing geophysical gradient in the data. It may be very useful to average out noise, but not at the sacrifice of geophysical gradient information. Using the structure results above, a distance can be determined at which the structure function (mean-squared gradient) increases above the noise level. By simulations of perfect gradients with added noise (Hillger et al., 1986), it was determined that gradient information is detectable in the structure functions at a level only 10% above the extrapolated structure (noise level). In other words, when the structure function reaches a value of 110% of its minimum, then the presence of a gradient is apparent above the noise.

Table 7 gives the distances at which the structure functions showed detectable gradient. This was determined using the same polynomials that were used to extrapolate to zero distance for the estimated noise levels. The gradient was assumed to be detectable when the polynomial value increased by 10% above its minimum (intercept) value. The computed distances seem reasonable when the structure plots and polynomials are examined. Table 7 also gives the distances to detectable gradient in terms of the number of fields of view (FOVs) that the distance represents. The results indicate that for the upper-tropospheric and stratospheric channels (VAS 1–3) the mean gradient is detectable only at a large distance, implying that the geophysical gradient is weak. The opposite is true for the lower tropospheric and near-surface channels (VAS 5–8 and 12) which have large gradient and show increasing structure even at small distances.

The results in Table 7 imply that spatial averaging is possible for measurements from many of the upper-tropospheric and stratospheric VAS channels without destroying gradient information in the process. However, averaging is not possible for the lower-tropospheric and surface channels without destroying gradient information. Since these results are gradient and dataset (spin budget) dependent, similar results should be computed on particular datasets of interest to the user.

TABLE 7. Distance and number of FOVs to detectable gradient (defined in text) of GOES-5 VAS effective blackbody temperatures for 7 Sep 1983 (1132 FOVs).

		Distance to detectable gradient		Number of FOVs	
VAS channel	Wavelength (μm)	line (km)	element (km)	line	element
1	14.7	267	175	11	12
2	14.5	220	92	7	3
3	14.3	112	156	8	3
4	14.0	117	47	3	3
5	13.3	<14	<23	1	1
6	4.5	31	<23	1	1
7	12.7	<14	<23	1	1
8	11.2	<14	<23	1	1
9	7.3	29	26	2	2
10	6.8	18	<23	2	2
11	4.4	na*	na	na	na
12	3.9	<14	<23	1	1

* na data not available.

b. Necessary averaging

Another way to look at the noise levels of satellite measurements is to compare them to the accuracy *necessary* for a specific use of the measurements. In the case of VAS performance, prelaunch sounding specifications (absolute rms errors) were established based on the need for accurate temperature and water vapor profile retrievals. The specified rms accuracies are much smaller than the single FOV noise levels of VAS. The result is that in most channels the measurements from many FOVs need to be averaged together in order to reduce random noise to the required specifications.

The inflight single sample noise levels in Table 8 are the same as those in Table 6. Because the structure-estimated noise is slightly exaggerated from the single-sample noise, the later was chosen for comparison. The single-sample noise levels are compared to the more stringent sounding FOV accuracy (Chesters and Robinson, 1983). Since random noise is reduced by the square root of the number of samples in the average, the number of measurements that need to be included in the average is the square of the ratio of the single-sample noise to the specified channel accuracy (in radiance units). The second to the last column in Table 8 gives the number of FOVs that need to be averaged together in order to reduce the random noise to the given specifications. With the exception of channel 1 the required number of FOVs ranged from 1 to 11. An extremely large number of FOVs need to be included in the average for channel 1 (with peak contribution from the stratosphere). Three or more FOVs need to be averaged for nearly all channels in order to reduce their single-sample noise levels to the required accuracy for the use of the data. Spatial averaging is not necessary for VAS channel 8.

The second to the last column in Table 8 also shows the required number of FOVs divided into an approximate averaging area; however, no distinction is made between east–west and north–south orientations. These results indicate the amount of averaging necessary to obtain required noise levels, which is different than the possible averaging implied in Table 7. The last column in Table 8 qualitatively compares the required averaging from this table with the possible averaging from Table 7. One significant conclusion is that for channels which require averaging but which show gradient at high resolution (VAS 5–7 and 12), small-scale information is sacrificed to obtain the required absolute accuracy. On the other hand, when more averaging is possible than is required for accuracy considerations (especially VAS 1–3), the extra averaging will result in lower noise and in the saving of analysis time for data which has little or no detectable geophysical gradient information. Other channels (VAS 4 and 8–10) neither lose information nor gain by additional averaging, since the required and possible averaging are approximately equal. Thus, a user of these satellite data is presented with a choice. If the user's primary purpose is to detect geophysical gradient (e.g. thermal or moisture features of discontinuity) then the amount of possible averaging is to be favored. If, however, the absolute geophysical values are required, then additional averaging may be necessary.

Others have employed averaging techniques to improve retrieved products from VAS measurements. Smith et al. (1985) derived total precipitable water and atmospheric stability from VAS at both 7 and 80 km resolution. The conclusion was that although the higher resolution values appear noisy, coherent small-scale features can be seen. This agrees with the fact that some spatial averaging is needed but that high-resolution information does exist in most of the low-level VAS channels. Likewise, Chesters et al. (1986) and Robinson et al. (1986) found that VAS data produced the best retrievals of atmospheric parameters when the VAS

TABLE 8. Required averaging of GOES-5 VAS channels to meet absolute sounding FOV accuracy.

VAS channel	Wavelength (μm)	Inflight SSN* (K)	Sounding FOV accuracy** (K)	Required number of FOVs	Loss of information***
1	14.7	2.28	0.3	64 (~8 × 8)	No
2	14.5	0.93	0.3	11 (~4 × 3)	No
3	14.3	0.64	0.3	6 (~3 × 2)	No
4	14.0	0.52	0.2	6 (~3 × 2)	No
5	13.3	0.40	0.2	6 (~3 × 2)	Yes
6	4.5	0.22	0.1	8 (~3 × 3)	Yes
7	12.7	0.28	0.2	4 (~2 × 2)	Yes
8	11.2	0.06	0.2	1 (~1 × 1)	No
9	7.3	0.83	0.4	6 (~3 × 2)	No
10	6.8	0.72	0.5	3 (~2 × 2)	No
11	4.4	1.95	0.3	43 (~7 × 7)	na†
12	3.9	0.19	0.1	4 (~2 × 2)	Yes

* SSN: single sample noise from Table 6.
** Sounding FOV absolute rms errors to be obtained by spatial averaging (Chesters and Robinson, 1983).
*** When comparing necessary averaging to possible averaging from Table 7.
† Data not available.

measurements were averaged to 30–60 km resolution at low levels and 60–120 km at middle levels. This is equivalent to averaging 2 to 4 and 4 to 6 FOVs, respectively. This is a compromise between noisy single FOV values and loss of information by too much averaging; it also confirms that spatial averaging can vary with height or channel. The averaging volume for VAS channels should appear more like a cone than a cylinder, with additional averaging at higher levels.

6. Summary and conclusions

Statistical structure analysis provides a means of estimating the noise level in remotely sensed measurements from satellites. The structure is a measure of the mean gradient plus noise in the analyzed data. Separation of the gradient from the noise is possible by extrapolating the structure function to zero distance. This is accomplished by fitting various polynomials to the discrete structure values. The remaining structure after extrapolation is twice the mean-squared noise.

Structure analysis was applied to spatial arrays of measurements from four satellite sounding instruments. The structure-estimated noise levels were compared to either prelaunch specifications or inflight calibrations. Agreements were generally within a factor of 2 (noise ratios ranging from 0.5 to 2.0) for measurements which were not affected by clouds or ground surface variations. Clouds were a problem for infrared measurements, especially those from the lower troposphere and the surface. In those cases, structure analysis overestimated the noise level, so use of cloud-free data is recommended. Variations in results for noncloud contaminated channels may be due to an insufficient sample size in this study or due to nonrepresentativeness of the specifications or calibration data. Results presented here are used mainly to illustrate this technique and are not meant to be the final word on any of the instruments analyzed.

Microwave remote sensing measurements are generally not affected by clouds, so the estimation of noise levels is easier using data from the microwave part of the spectrum. Structure-estimated noise was within prelaunch specifications for all but the microwave window channels, which are affected by high-resolution surface emittance variations. Structure analysis, therefore, is a statistical means of estimating the noise level of operational satellite measurements, provided that care is taken to avoid cloud- or surface-contaminated measurements and that the data sample is sufficiently large.

Finally, the estimated noise levels can be interpreted in terms of what they imply about spatial averaging of the analyzed data from a user point of view. One interpretation is the result of determining the distance at which gradient information is detectable above the noise level. This indicates the averaging *possible* before gradient information is destroyed. The other interpretation is the result of comparing the estimated noise levels to the required accuracy for the use of the satellite measurements in a particular situation. This comparison indicates the amount of spatial averaging *necessary* to reduce the random noise in the measurements to given specifications. Data users will benefit from considering both interpretations and should recognize and take advantage of the choice of averaging options.

Acknowledgments. The satellite data used in this study were obtained from the NOAA/NESDIS Satellite Applications Laboratory at the University of Wisconsin. Mr. Alan Lipton provided helpful suggestions and a review of the manuscript. Ms. Bobbie Schwinger ably typed the manuscript. This work was funded under NOAA Grant NA85RAH05045 and NASA Contract NAS8-36472.

REFERENCES

Aerojet ElectroSystems Company, 1977: System summary report—Passive Microwave Sounder (SSM/T). Prepared for USAF Space and Missile Systems Organization, Defense Meteorological Satellite Program, Los Angeles, 139 pp.

Chesters, D., and W. D. Robinson, 1983: Performance appraisal of VAS radiometry for GOES-4, -5, and -6. NASA Tech. Memo. 85125, NASA-GSFC, 55 pp.

——, A. Mostek and D. A. Keyser, 1986: VAS sounding images of atmospheric stability parameters. *Wea. Forecasting,* **1,** 5–22.

Fuelberg, H. E., and P. J. Meyer, 1986: An analysis of mesoscale VAS retrievals using statistical structure functions. *J. Climate Appl. Meteor.,* **25,** 59–75.

Gandin, L. S., 1963: *Objective Analysis of Meteorological Fields.* Translated from Russian, Israel Program for Scientific Translations, Jerusalem, 242 pp. [NTIS: TT-65-50007.]

Grody, N. C., D. G. Gray, C. S. Novak, J. S. Prasad, M. Piepgrass and S. A. Dean, 1985: Temperature sounding from the DMSP microwave sounder. *Advances in Remote Sensing Retrieval Methods,* A. Deepak, H. E. Fleming, and M. T. Chahine, Eds., A. Deepak, 249–267.

Hillger, D. W., and T. H. Vonder Haar, 1979: An analysis of satellite infrared soundings at the mesoscale using statistical structure and correlation functions. *J. Atmos. Sci.,* **36,** 287–305.

——, J. F. W. Purdom and T. H. Vonder Haar, 1986: The use of structure function analysis to estimate noise levels and the potential resolution of satellite measurements. *Preprints, Second Conf. on Satellite Meteorology/Remote Sensing and Applications,* Williamsburg, Amer. Meteor. Soc., 102–107.

Menzel, W. P., W. L. Smith, G. S. Wade, L. D. Herman and C. M. Hayden, 1983: Atmospheric soundings from a geostationary satellite. *Appl. Opt.,* **22,** 2686–2689.

Robinson, W. D., D. Chesters and L. W. Uccellini, 1986: Optimized retrievals of precipitable water fields from combinations of VAS satellite and conventional surface observations. *J. Geophys. Res.,* **91,** 5305–5318.

Schwalb, A., 1978: The TIROS-N/NOAA A-G satellite series. NOAA Tech. Memo., NESS 95, 75 pp. [NTIS: PB-283859.]

Smith, W. L., 1983: The retrieval of atmospheric profiles from VAS geostationary radiance observations. *J. Atmos. Sci.,* **40,** 2025–2035.

——, G. S. Wade and H. M. Woolf, 1985: Combined atmospheric sounding/cloud imagery—a new forecasting tool. *Bull. Amer. Meteor. Soc.,* **66,** 138–141.

Swanson, P. N., W. M. Harris, E. J. Johnston and F. S. Soltis, 1980: The TIROS-N Microwave Sounder Unit. *IEEE MTT-S International Microwave Symposium Digest,* 123–125.

Werbowetzki, A. (Ed.), 1981: Atmospheric Sounding User's Guide. NOAA Tech. Rep., NESS 83, 82 pp. [NTIS: PB81-230476.]